IEEE Access
Multidisciplinary ⋮ Rapid Review ⋮ Open Access Journal

Received October 19, 2021, accepted November 24, 2021, date of publication November 25, 2021,
date of current version December 10, 2021.

Digital Object Identifier 10.1109/ACCESS.2021.3131061

A Nonlinear MIMO-OFDM Based Full-Duplex Cooperative D2D Communications System

MANISH DASH[1], RAHUL BAJPAI[1], NAVEEN GUPTA[1], AND PARAG AGGARWAL[2], (Member, IEEE)

[1]Department of Electrical and Electronics Engineering, BITS Pilani, K. K. Birla Goa Campus, Zuarinagar, Goa 403726, India
[2]5G Research and Development Laboratory, HFCL Ltd., Gurugram 122001, India

Corresponding author: Rahul Bajpai (p20190003@goa.bits-pilani.ac.in)

ABSTRACT Multiple input multiple output (MIMO) based orthogonal frequency division multiplexing (OFDM) has widely been used in a wireless communications system for its robustness to frequency-selective channels and better spectral efficiency. The introduction of full-duplex (FD) and device-to-device (D2D) communications, which are potential candidates of fifth-generation (5G) and beyond, further improve the spectral efficiency of MIMO-OFDM based systems. This paper proposes a novel MIMO-OFDM based FD Cooperative-D2D (C-D2D) communications system wherein a cellular user (CU) acts as an FD relay to facilitate seamless communications between D2D transmitter and receiver. The complete analytical framework is presented to analyze the end-to-end performance of the proposed system. Specifically, the closed-form expression for symbol error rate (SER) of the proposed system is derived in the presence of multipath Rayleigh fading channel and residual self-interference (RSI) due to the FD mode. Further, the performance of the system is analyzed in the presence of a nonlinear high power amplifier (HPA) which introduces the nonlinear distortion. Finally, simulation results are presented to verify the derived expressions. The results show that there is higher SER in the presence of nonlinear HPA due to nonlinear distortion, which can be reduced by increasing input back off (IBO). The presence of RSI also increases the SER at CU, which is further reduced by employing self-interference cancellation (SIC) techniques. A complete end-to-end analytical framework is designed to compare the performance of the proposed system with the conventional system with linear HPA and no RSI.

INDEX TERMS Cooperative device-to-device communication, full-duplex, high power amplifier, nonlinear distortion, residual self-interference.

I. INTRODUCTION

With the rapid proliferation of the internet of everything (IoE) systems [1], [2] connecting billions of machines and millions of mobile devices, the need for ultra-high data rates have increased by leaps and bounds. The fifth-generation (5G) and beyond cellular networks are expected to provide ultra-high data rate, and large user capacity to fulfill the requirements of IoE applications with low latency and enhanced reliability [3]–[5]. Some of the promising technologies of 5G and beyond cellular networks, such as device-to-device (D2D) communications, full-duplex (FD) radios, provide higher capacity, lower latency, and better spectral efficiency (SE) as compared to the existing cellular networks.

The associate editor coordinating the review of this manuscript and approving it for publication was Luyu Zhao.

D2D communication is one of the promising technologies for 5G and beyond cellular networks due to its capability to allow data transmission among two or more cellular users (CUs) in proximity without or a limited involvement of a base station (BS) [6]. However, BS still monitors the signaling and control information [7]. D2D communication improves both SE and energy efficiency (EE) of the 5G and beyond cellular networks [8]. D2D users coexist with other CUs by adopting one of the three possible frameworks: underlay, overlay, or cooperative-D2D (C-D2D). In [9], authors have shown that the C-D2D framework dominates in terms of quality-of-service (QoS) for both CUs and D2D users as compared to the underlay and overlay frameworks. In the C-D2D framework, a relay is utilized for cellular or D2D transmission for achieving the desired QoS between the source and destination. Regardless of lesser signal processing capability than

a BS, user equipment, such as a CU, can be used as a relay instead of a BS for a C-D2D system [10]. Usage of CU as a relay provides an additional advantage in reducing the infrastructural cost incurred and power consumption, compared to the case when a BS would be used as a relay [11].

FD radios can simultaneously transmit and receive (STAR) signals over the same time-frequency resource block and hence can achieve double SE as compared to half-duplex (HD) radios [12]. However, STAR deteriorates the performance of the FD system due to the occurrence of self-interference (SI). Authors in [13]–[16] have shown that by utilizing active and passive SI cancellation (SIC) schemes, the impact of SI can be reduced significantly. However, in practical FD systems, SI cannot be mitigated completely, and there is always some residual SI (RSI) present in the system [17]. The SE of a communication system can be further enhanced, when FD mode is integrated with the C-D2D framework [12], [18].

The FD based C-D2D system can be further extended to include orthogonal frequency division multiplexing (OFDM), which can provide robustness to the system towards multipath and frequency selective channel. In [19], the authors have utilized the prospective advantages of OFDM in FD C-D2D systems to improve the outage performance. Further, MIMO is another core technology that helps to achieve better SE and EE when integrated with OFDM [20]. The integration of MIMO-OFDM with FD C-D2D communication system can enhance the SE with improved reliability of the transmission. Since OFDM suffers from a high peak to average power ratio (PAPR), the usage of HPA limits the performance of the OFDM based system by introducing the nonlinear distortion [21]. However, increasing the input back-off (IBO) is a prominent scheme that can be used for mitigating the non-linearity effect introduced by the HPAs [22].

A. RELATED WORKS

In [23], authors have proposed an FD C-D2D system wherein a CU acts as an FD decode-and-forward (DF) relay for D2D transmission. Further, two optimal power allocations schemes are investigated to maximize the minimum achievable rate and minimize the joint outage probability. Similarly, in [24], the authors have proposed an FD relay-assisted D2D communications system with orthogonal frequency division multiple access (OFDMA), wherein two relay selection schemes: bulk selection and per subcarrier selection, are compared. The closed-form expressions of outage probabilities have been derived and verified numerically. However, the work in [23], [24] is limited to single carrier transmissions with a maximum of two antennas at CU, and the performance gain due to MIMO-OFDM has not been explored.

In [25], [26], the authors have proposed an OFDMA based FD C-D2D based system, wherein a D2D transmitter (DT) acts as a DF relay for cellular uplink/downlink communications. The authors have derived the analytical expressions of D2D and cellular outage probabilities to analyze the performance of C-D2D systems. Similarly, in [27], the authors have obtained the average achievable rate of D2D transmission and the outage probability of a CU for a C-D2D system. Further, the authors have also obtained optimal power and spectrum allocation to maximize the total average achievable rate. However, the analysis in [24]–[27] are based on a single input single output (SISO) system, and the performance gain due to multi-antenna techniques has not been explored. In [28], authors have proposed a D2D MIMO communications system, wherein a D2D user acts as an amplify-and-forward (AF) relay for the cellular downlink transmission. Further, the best antenna selection scheme has been adopted to maximize the received power at the destination node. Additionally, the analytical expression of ergodic capacity has been derived and verified through the simulations. However, the analysis is limited to HD relaying and single-carrier transmissions. The prospective advantages of FD relaying with OFDM are not explored.

In [29], authors have proposed a frequency division duplexing (FDD) based massive MIMO system with D2D enabled user cooperation to maximize the utility function. Further, two D2D-enabled user cooperation schemes are proposed, which include receive-signal-information and the data-symbol-information exchanging. However, the proposed system model has not included multicarrier transmission. Furthermore, the works mentioned above do not consider the nonlinear distortion due to the presence of HPAs.

In [30], [31], the authors have highlighted the impact of a nonlinear HPA on a multi-user (MU) MIMO-OFDM system. Further, in [31], the authors have derived the signal to distortion noise ratio (SDNR) for each user in each subcarrier for a general power allocation and linear precoding scheme at the BS. In [32], the authors have done an end-to-end analysis of the impact of a nonlinear transmitter on a carrier aggregated (CA) MU-MIMO-OFDM system. However, the analysis in [30]–[32] is limited to the HD system, and the benefits of FD mode are not explored. In addition, the MU-MIMO-OFDM has not been tested for a D2D environment.

A MIMO system with FD relay (FDR) is proposed in [33]. The performance of the system is analyzed in terms of SER in the presence of the channel estimation error (CEE), transceiver hardware impairment (THI), and RSI. However, the system model has not considered MIMO-OFDM and impairments due to non-linear HPA. In [34], [35], the authors have studied the impact of nonlinear devices on OFDMA signals and analytically evaluated the effects of nonlinear distortion. Similarly, [36], [37] describes the nonlinear MIMO-OFDM systems wherein the spectral characteristics of the nonlinear distortion term have been discussed. However, the analysis presented in [34]–[37] is limited to the impact of nonlinear distortions in MIMO-OFDM system. The effect of nonlinear distortions has not been explored for the FD C-D2D communications system. To the best of the authors' knowledge, the performance of an FD system in the presence of a non-linear HPA has not been studied yet. Further, the performance of the MIMO-OFDM based

FD C-D2D system in the presence of non-linear HPA has also not been explored yet.

B. CONTRIBUTIONS

Motivated by the existing literature, in this paper, we have proposed a MIMO-OFDM based FD C-D2D communications system, where a CU assists D2D transmission. Our major contributions are summarized as follows:

- A complete end-to-end analytical methodology is proposed to obtain the received SDNR and symbol error rate (SER) of the proposed MIMO-OFDM based FD C-D2D communications system.
- The performance of the proposed MIMO-OFDM based FD C-D2D communications system with non-linear HPA and RSI is compared with the conventional MIMO-OFDM based FD C-D2D communications system with linear HPA and no RSI.
- The closed-form expressions of SER for both the D2D transmissions, i.e., between DT and CU and between CU and D2D receiver (DR) have been derived.
- Impact of the RSI parameters on SER of linear MIMO-OFDM based FD C-D2D system is investigated. It is shown that the SER degrades with the increase in the RSI parameters.

The rest of the paper is organized as follows. Section II shows the proposed MIMO-OFDM FD C-D2D system model. Section III shows the mathematical analysis of a linear MIMO-OFDM FD C-D2D system, and Section IV illustrates the detailed mathematical analysis of non-linear MIMO-OFDM FD C-D2D. Section V shows the simulation results, and in the end, this paper has been concluded in Section VI.

Notations:

- Matrices have been denoted by upper case bold-face non-italic letters.
- Vectors have been denoted by lower case bold-face non-italic letters with an overline.
- Scalars have been denoted by lower case non-bold italic letters.

II. SYSTEM MODEL

As shown in Fig. 1, we have considered a cell having a BS, a D2D pair, and a CU. Further, we consider that there is no direct link available between DT and DR due to heavy shadowing or the presence of physical hindrances [23]. CU working in FD mode acts as a DF relay for the D2D transmission. We consider DT consists of T_S transmit antennas, DR has T_D receive antennas, and CU has T_R transmit and receive antennas. $\mathbf{H_{SC}}$ and $\mathbf{H_{CD}}$ are Rayleigh fading MIMO channels between DT-CU and CU-DR, respectively. All the symbols and variables used in this paper are listed in Table 1.

The OFDM modulator block on a transmitter side has a serial to parallel converter block, followed by an M-QAM modulator, an inverse discrete Fourier transform (IDFT) block, cyclic prefix (CP) insertion, and parallel to serial conversion. The output of the OFDM modulator is sent as input to the HPA.

The OFDM modulator block and the HPA block at the transmitter side of DT have been shown in Fig. 2. As shown in Fig. 2 and Fig. 3, the receiver side at CU and DR consists

TABLE 1. Description of variables and operations.

Variables or, Operations	Description
$\mathrm{E}[\cdot]$	Expectation operator
$(\cdot)^{\dagger}$	Pseudo inverse operator
$(\cdot)^{*}$	Conjugate operator
$(\cdot)^{H}$	Hermitian operator
$(\cdot)^{-1}$	Inverse operator
$\mathrm{Q}(\cdot)$	Q function
$\mathcal{CN}(m,\sigma^2)$	Complex Gaussian distribution with mean m and variance σ^2
T_S	Number of transmit antennas at DT
T_R	Number of transmit and receive antennas at CU
T_D	Number of receive antennas at DR
N	Number of OFDM subcarriers
N_{CP}	Length of CP
$\mathbf{H_{AB}[n]}$	Rayleigh fading MIMO channel matrix between A and B
$\hat{h}_{AB_{r,t,k}}$	Effective channel coefficient between t^{th} transmit antenna of A and r^{th} receive antenna of B of the k^{th} subcarrier
$\mathbf{\hat{H}_{AB}(k)}$	Frequency domain equivalent MIMO channel matrix at k^{th} subcarrier between A and B whose elements are $\hat{h}_{AB_{r,t,k}}$
d_{AB}	Distance between A and B
β, λ	Parameters determing the performance of SIC
P_s	Transmit Power at DT
P_c	Transmit Power at CU
$\eta_{AB}(k)$	Effective complex data symbol for C-D2D transmission between A and B using linear HPA
$\zeta_{AB}(k)$	Effective complex data symbol for C-D2D transmission between A and B using non-linear HPA
μ_{AB_t}	Multiplicative gain from non-linear HPA at A when transmitting to B
γ_{AB_t}	Additive residual noise from non-linear HPA at A when transmitting to B
$\overline{\mathbf{q}}_{\mathbf{c}}[\mathbf{n}], \overline{\mathbf{q}}_{\mathbf{D}}[\mathbf{n}]$	Received signal vectors at CU and DR respectively
$\overline{\mathbf{v}}_{\mathbf{c}}[\mathbf{n}]$	RSI vector at CU
$\overline{\mathbf{w}}_{\mathbf{c}}[\mathbf{n}], \overline{\mathbf{w}}_{\mathbf{D}}[\mathbf{n}]$	AWGN vectors at CU and DR respectively
$\rho_{t_{AB}}(k)$	SDNR between A and B at k^{th} sub-carrier
$f_{t_{AB}}(k)(\psi_k)$	SER between A and B

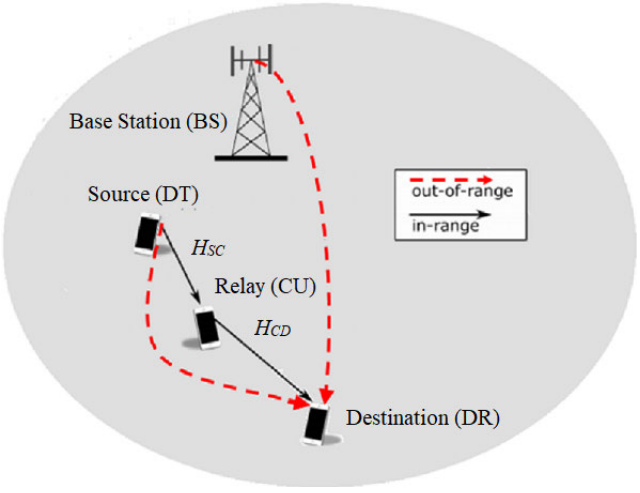

FIGURE 1. System model.

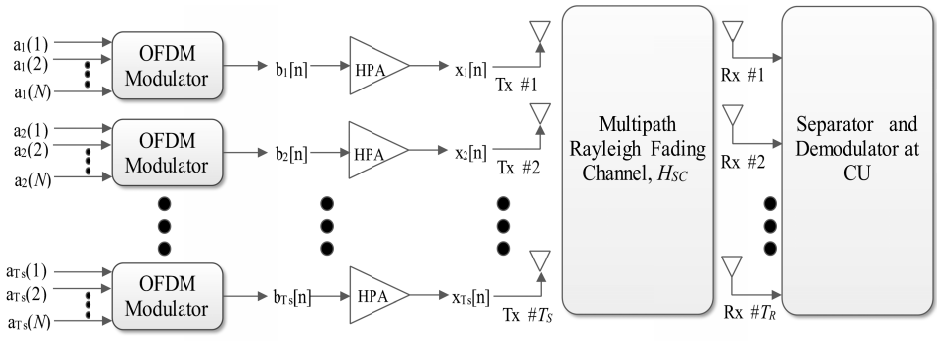

FIGURE 2. Non-linear MIMO-OFDM model from DT to CU.

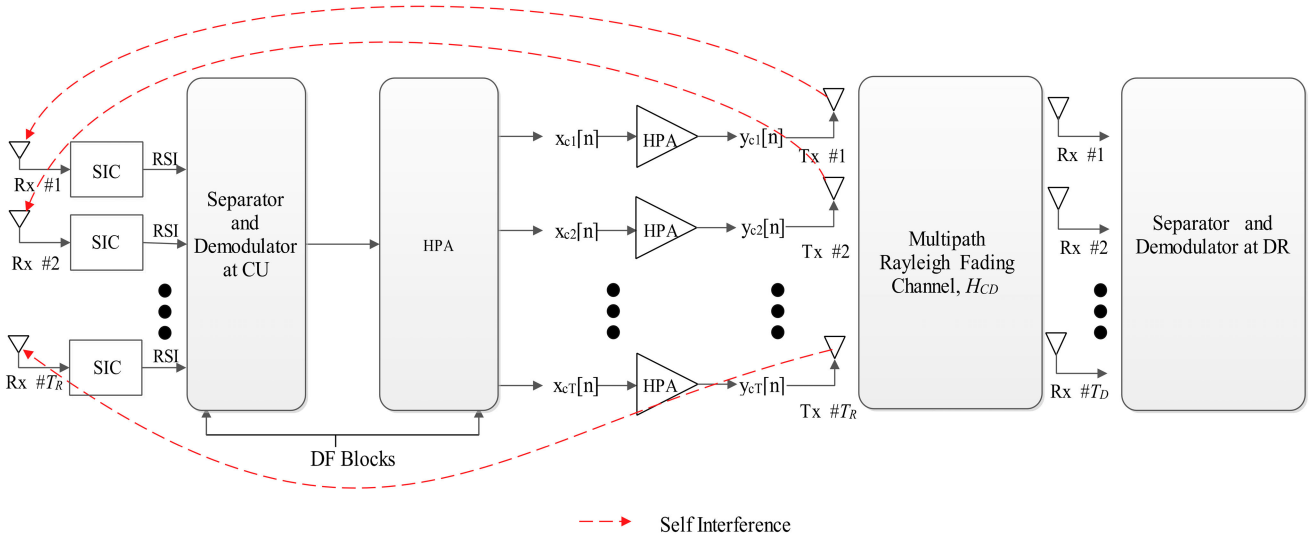

FIGURE 3. Non-linear MIMO-OFDM Model from CU to DR.

of the serial to parallel conversion, followed by CP removal, discrete Fourier transform (DFT), M-QAM demodulator, and parallel to serial converter. Further, as shown in Fig. 3, the receiver side of CU has an additional SIC block for canceling the SI received from the transmitter side of CU. The RSI and the AWGN at the receiver at CU are added to the received signal. The signal from DT is demodulated and decoded at the receiver end of CU before forwarding it to the transmitter side of the CU for relaying the data to DR. The OFDM symbol generation on the transmitter side at DT is represented as:

$$b_t[n] = \begin{cases} \frac{1}{N}\sum_{k=0}^{N-1} a_t(k)\sqrt{P_s}e^{\frac{j2\pi kn}{N}} & -N_{CP} \le n \le N-1 \\ 0; & \text{otherwise.} \end{cases} \tag{1}$$

Here, $b_t[n]$ is the OFDM symbol input to HPA on the t^{th} transmit antennas at DT and $a_t(k)$ is a set of independent and identically distributed (i.i.d) complex data symbols with zero mean and variance P_s on the t^{th} transmit antenna. Using central limit theorem [38], for large N, $b_t[n]$ can be considered to be a random variable following a complex Gaussian distribution with zero mean and variance, $P_{av} = \frac{P_s}{N}$.

The multipath Rayleigh fading channel between node A and B, where, $A \in \{S, C\}$ and $B \in \{C, D\}$,[1] can be modeled as:

$$\mathbf{H_{AB}[n]} = \sum_{\omega=1}^{\Omega_f} \mathbf{H_{f_\omega}} \delta[n-\omega], \tag{2}$$

where, $f = \{1, 2\}$ for the transmission between DT and CU and for transmission between CU and DR respectively, Ω_f is the number of delay taps, and $\mathbf{H_{f_\omega}}$ contains the MIMO channel coefficients for the ω^{th} multipath between A and B, which can be written as:

$$\mathbf{H_{f_\omega}} = \begin{bmatrix} h_{AB_{1,1,\omega}} & h_{AB_{1,2,\omega}} & . & . & h_{AB_{1,K,\omega}} \\ h_{AB_{2,1,\omega}} & h_{AB_{2,2,\omega}} & . & . & h_{AB_{2,K,\omega}} \\ . & . & . & . & . \\ . & . & . & . & . \\ . & . & . & . & . \\ h_{AB_{J,1,\omega}} & h_{AB_{J,2,\omega}} & . & . & h_{AB_{J,K,\omega}} \end{bmatrix}_{J\times K}, \tag{3}$$

where, $J \in \{T_R, T_D\}$ denoting the number of receive antennas, $K \in \{T_S, T_R\}$ denoting the number of transmit antennas

[1]For the simplification of notations, we have represented CU, DT, and DR as C, S, and D respectively.

and $h_{AB_{r,t,\omega}}$ is the channel impulse response between the t^{th} transmit antenna at DT and the r^{th} receive antenna at CU for the ω^{th} delay tap, which are i.i.d and follow $\mathcal{CN}(0, 1)$. The channel coefficients vary as the distance between A and B changes.

In our proposed model, the nonlinear distortion and RSI are modeled as a Gaussian random variable. In [39], [40], it has been mathematically shown that the nonlinear distortion can be expressed in terms of Gaussian random variable. Further, as we are considering FD relay instead of HD, there will be an additional SI term at the FD node CU. Most of the current research in FD systems considers that after active and passive cancellation of SI, the RSI can be modeled as a Gaussian random variable according to the central limit theorem [41]–[43]. Hence, motivated by the above, we have modeled the nonlinear distortion due to HPA and the RSI term as a Gaussian random variable in our proposed MIMO-OFDM based FD C-D2D system. Each element in RSI at CU follows $\mathcal{CN}(0, \beta P_c^{\lambda})$, where P_c is the transmit power of the message sent by CU to DR, $\beta \in [0, \infty)$ and $\lambda \in (0, 1)$. β and λ are parameters which determine the performance of the SIC [23].

III. SDNR CALCULATIONS WITH LINEAR HPAs

This section consists of the SDNR calculations between the links DT-CU and CU-DR for our proposed MIMO-OFDM based FD C-D2D communications system.

A. BETWEEN DT AND CU

We have considered multipath Rayleigh fading channel H_{SC} between DT and CU. Linear HPAs are assumed to be present at each transmit antenna with unit power. DT transmits a signal to CU, which utilizes DF protocol before forwarding it to DR. The received signal vector $\overline{\mathbf{q}}_{\mathbf{c}}[\mathbf{n}]$ at CU is given by,

$$\overline{\mathbf{q}}_{\mathbf{c}}[\mathbf{n}] = \mathbf{H}_{\mathbf{1}_{\omega}}[\mathbf{n}]\overline{\mathbf{b}}[\mathbf{n} - \omega] + \overline{\mathbf{v}}_{\mathbf{c}}[\mathbf{n}] + \overline{\mathbf{w}}_{\mathbf{c}}[\mathbf{n}]. \tag{4}$$

Here, $\overline{\mathbf{q}}_{\mathbf{c}}[\mathbf{n}]$ is a $T_R \times 1$ vector of receive signals, $\overline{\mathbf{b}}[\mathbf{n}]$ is the $T_S \times 1$ vector of transmitted signals from HPA at DT, $\overline{\mathbf{v}}_{\mathbf{c}}[\mathbf{n}]$ is a $T_R \times 1$ vector for RSI at CU, and $\overline{\mathbf{w}}_{\mathbf{c}}[\mathbf{n}]$ is a $T_R \times 1$ for AWGN at CU where each element follows $\mathcal{CN}(0, N_o)$.

The complex data symbol received at the r^{th} receive antenna is written as

$$q_{c_r}[n] = \sum_{t=0}^{T_S-1}\sum_{\omega=0}^{\Omega_1-1} h_{SC_{r,t,\omega}}\overline{\mathbf{b}}[\mathbf{n} - \omega] + v_{c_r}[n] + w_{c_r}[n]. \tag{5}$$

After the removal of the CP and applying DFT,

$$\begin{aligned} q_{c_r}(k) &= \sum_{n=0}^{N-1} q_{c_r}[n]e^{\frac{-j2\pi kn}{N}}, \\ &= \sum_{n=0}^{N-1}\sum_{t=0}^{T_S-1}\sum_{\omega=0}^{\Omega_1-1} h_{SC_{r,t,\omega}}\overline{\mathbf{b}}[\mathbf{n} - \omega]e^{\frac{-j2\pi kn}{N}} \\ &\quad + v_{c_r}(k) + w_{c_r}(k). \end{aligned} \tag{6}$$

Using circular shift property of DFT,

$$\begin{aligned} q_{c_r}(k) &= \sum_{t=0}^{T_S-1}\sum_{\omega=0}^{\Omega_1-1} h_{SC_{r,t,\omega}}\sum_{n=0}^{N-1}\overline{\mathbf{b}}[\mathbf{n}]e^{\frac{-2\pi k(n+\omega)}{N}} \\ &\quad + v_{c_r}(k) + w_{c_r}(k), \\ &= \sum_{t=0}^{T_S-1}\hat{h}_{SC_{r,t,k}}\eta_{SC}(k) + v_{c_r}(k) + w_{c_r}(k), \end{aligned} \tag{7}$$

where, $\hat{h}_{SC_{r,t,k}}$ is the effective channel coefficient between t^{th} transmit antenna of DT and r^{th} receive antenna of CU of the k^{th} subcarrier, and given by

$$\hat{h}_{SC_{r,t,k}} = \sum_{\omega=0}^{\Omega_1-1} h_{SC_{r,t,\omega}}e^{\frac{-2\pi k\omega}{N}}. \tag{8}$$

Further, $\eta_{SC}(k)$ is the effective complex data symbol and is given by,

$$\eta_{SC}(k) = \sum_{n=0}^{N-1}\overline{\mathbf{b}}[\mathbf{n}]e^{\frac{-j2\pi kn}{N}}. \tag{9}$$

Hence, from (9)

$$\eta_{SC}(k) = a(k). \tag{10}$$

Thus,

$$q_{c_r}(k) = \sum_{t=0}^{T_S-1}\hat{h}_{SC_{r,t,k}}a(k) + v_{c_r}(k) + w_{c_r}(k). \tag{11}$$

Using zero forcing equalization, the complex data symbol at k^{th} subcarrier can be estimated as:

$$\hat{a}(k) = a(k) + [(\hat{\mathbf{H}}_{\mathbf{SC}}(\mathbf{k}))^{\dagger}(v_c(k) + w_c(k))]^t, \tag{12}$$

where, $\hat{a}(k)$ is the decoded symbol at CU at k^{th} subcarrier and $[(\hat{\mathbf{H}}_{\mathbf{SC}}(\mathbf{k}))^{\dagger}(v_c(k) + w_c(k))]^t$ denotes the t^{th} element of the vector, $[(\hat{\mathbf{H}}_{\mathbf{SC}}(\mathbf{k}))^{\dagger}(v_c(k) + w_c(k))]$.

SDNR for k^{th} subcarrier at CU is given by,

$$\begin{aligned} \rho_{t_{SC}}(k) &= \frac{P_s}{[((\mathbf{H_{SC}})^H\mathbf{H_{SC}})^{-1}]^t(N_o + \beta P_c^{\lambda})}, \\ &= \frac{P_s}{N_o + \beta P_c^{\lambda}}\psi_{SC}, \end{aligned} \tag{13}$$

where, ψ_{SC} is a random variable following Chi-squared distribution with $2(T_R - T_S + 1)$ degrees of freedom and given as,

$$\psi_{SC} = \frac{1}{[((\mathbf{H_{SC}})^H\mathbf{H_{SC}})^{-1}]^t}. \tag{14}$$

If the FD system is ideal without any RSI, then the SDNR becomes,

$$\rho_{SC}(k) = \frac{P_s}{N_o}\psi_{SC}. \tag{15}$$

B. BETWEEN CU AND DR

1) TRANSMIT SIGNAL AT CU

After decoding $\hat{a}(k)$, CU forms a broadcasting signal as

$$\bar{\mathbf{x}}_\mathbf{c}[\mathbf{n}] = \hat{\mathbf{a}}[\mathbf{n} - \mathbf{n_0}], \tag{16}$$

$\hat{\mathbf{a}}[\mathbf{n}]$ is the decoded message vector received from DT and n_o is the processing delay at CU. $\bar{\mathbf{x}}_\mathbf{c}[\mathbf{n}]$ is transmitted with power P_c.

2) RECEIVED SIGNAL CHARACTERISATION

The received signal vector $\bar{\mathbf{q}}_\mathbf{D}[\mathbf{n}]$ at DR, can be written as

$$\bar{\mathbf{q}}_\mathbf{D}[\mathbf{n}] = \mathbf{H}_{2_\delta}\bar{\mathbf{x}}_\mathbf{c}[\mathbf{n}] + \bar{\mathbf{w}}_\mathbf{D}[\mathbf{n}]. \tag{17}$$

Here, $\bar{\mathbf{w}}_\mathbf{D}[\mathbf{n}]$ is a $T_D \times 1$ vector of AWGN at DR, where each element follows $\mathcal{CN}(0, N_o)$.

The complex data symbol received at the r^{th} receive antenna at DR can be written as:

$$q_{D_r}[n] = \sum_{t=0}^{T_R-1}\sum_{\omega=0}^{\Omega_2-1} h_{CD_{r,t,\omega}}\bar{\mathbf{x}}_\mathbf{c}[\mathbf{n} - \omega] + w_{D_r}[n]. \tag{18}$$

After the removal of the CP and applying DFT,

$$\begin{aligned} q_{D_r}(k) &= \sum_{n=0}^{N-1} q_{D_r}[n]e^{\frac{-j2\pi kn}{N}}, \\ &= \sum_{n=0}^{N-1}\sum_{t=0}^{T_R-1}\sum_{\omega=0}^{\Omega_2-1} h_{CD_{r,t,\omega}}\bar{\mathbf{x}}_\mathbf{c}[\mathbf{n} - \omega]. \end{aligned} \tag{19}$$

On further solving,

$$q_{D_r}(k) = \sum_{n=0}^{N-1}\sum_{t=0}^{T_R-1}\sum_{\omega=0}^{\Omega_2-1} h_{CD_{r,t,\omega}}\bar{\mathbf{x}}_\mathbf{c}[\mathbf{n} - \omega]e^{\frac{-j2\pi kn}{N}} + w_{D_r}(k). \tag{20}$$

Using circular shift property of DFT,

$$\begin{aligned} q_{D_r}(k) &= \sum_{t=0}^{T_R-1}\sum_{\omega=0}^{\Omega_2-1} h_{CD_{r,t,\omega}}\sum_{n=0}^{N-1}\bar{\mathbf{x}}_\mathbf{c}[\mathbf{n}]e^{\frac{-2\pi k(n+\omega)}{N}} + w_{D_r}(k), \\ &= \sum_{t=0}^{T_R-1}\hat{h}_{CD_{r,t,k}}\eta_{CD}(k) + w_{D_r}(k), \end{aligned} \tag{21}$$

where, $\hat{h}_{CD_{r,t,k}}$ is the effective channel coefficient between t^{th} transmit antenna of CU and r^{th} receive antenna of DR of k^{th} subcarrier. $\eta_{CD}(k)$ is the effective complex data symbol and is given by,

$$\eta_{CD}(k) = \sum_{n=0}^{N-1}\bar{\mathbf{x}}_\mathbf{c}[\mathbf{n}]e^{\frac{-j2\pi kn}{N}}, \tag{22}$$

If the processing delay is negligible, then $\eta_{CD_t}(k)$ can also be written as,

$$\eta_{CD}(k) = \hat{a}(k). \tag{23}$$

Thus,

$$q_{D_r}(k) = \sum_{t=0}^{T_D-1}\hat{h}_{CD_{r,t,k}}\hat{a}(k) + w_{D_r}(k). \tag{24}$$

Using zero forcing equalization, the t^{th} complex data symbol at k^{th} subcarrier can be estimated as:

$$\tilde{a}(k) = \hat{a}(k) + [(\hat{\mathbf{H}}_\mathbf{CD}(\mathbf{k}))^\dagger w_D(k)]^t, \tag{25}$$

where, $\tilde{a}(k)$ is the decoded symbol at DR and $[(\hat{\mathbf{H}}_\mathbf{CD}(\mathbf{k}))^\dagger w_D(k)]^t$ denotes the t^{th} element of the vector, $[(\hat{\mathbf{H}}_\mathbf{CD}(\mathbf{k}))^\dagger w_D(k)]$.

SDNR between CU and DR is:

$$\begin{aligned} \rho_{t_{CD}}(k) &= \frac{P_c}{[((\mathbf{H_{CD}})^H\mathbf{H_{CD}})^{-1}]^t N_o}, \\ &= \frac{P_c}{N_o}\psi_{CD}. \end{aligned} \tag{26}$$

where, ψ_{CD} is a random variable following Chi-squared distribution with $2(T_D - T_R + 1)$ degrees of freedom and given as,

$$\psi_{CD} = \frac{1}{[((\mathbf{H_{CD}})^H\mathbf{H_{CD}})^{-1}]^T}. \tag{27}$$

SER for transmission between a node A and node B as approximated in [22] is given as:

$$f_{t_{AB}}(k)(\psi_k) \approx 4\left(1 - \frac{1}{\sqrt{M}}\right)\mathrm{Q}\left(\sqrt{\frac{3\rho_{t_{AB}}(k)}{(M-1)}}\right). \tag{28}$$

IV. SDNR CALCULATIONS WITH NON-LINEAR HPAs

This section analyzes the non-linearity effects introduced in the MIMO-OFDM based FD C-D2D system with a non-linear HPA.

A. BETWEEN DT AND CU

In this section, we evaluate the performance of a C-D2D FD non-linear MIMO-OFDM system in the presence of multi-path Rayleigh fading channel $\mathbf{H_{SC}}$. The non-linearity introduced by HPA at the t^{th} transmit antenna to the OFDM modulated signal $b_t[n]$, is represented by a non-linear polynomial $x_t[n]$ as shown in [22],

$$x_t[n] = \sum_{c_1=1}^{C_1}\alpha^t_{2c_1-1}\bar{b}_t[n]|b_t[n]|^{2(c_1-1)}. \tag{29}$$

C_1 is the non-linearity order and the coefficient of non-linearity for HPA for $(2c_1 - 1)^{th}$ order of non-linearity in the t^{th} transmit antenna is given by $\alpha^t_{2c_1-1}$.

The received signal vector $\bar{\mathbf{q}}_\mathbf{c}[\mathbf{n}]$ at CU is given by,

$$\bar{\mathbf{q}}_\mathbf{c}[\mathbf{n}] = \mathbf{H}_{\mathbf{1}_\omega}[\mathbf{n}]\bar{\mathbf{x}}[\mathbf{n} - \omega] + \bar{\mathbf{v}}_\mathbf{c}[\mathbf{n}] + \bar{\mathbf{w}}_\mathbf{c}[\mathbf{n}]. \tag{30}$$

The complex data symbol received at the r^{th} receive antenna can be written as

$$\begin{aligned} q_{c_r}[n] = &\sum_{t=0}^{T_S-1}\sum_{\omega=0}^{\Omega_1-1}\sum_{c=1}^{C_1} h_{SC_{r,t,\omega}}\alpha^t_{2c_1-1}b[n-\omega]|b[n-\omega]|^{2(c-1)} \\ &+ v_{c_r}[n] + w_{c_r}[n]. \end{aligned} \tag{31}$$

After the removal of the CP and applying DFT,

$$\begin{aligned} & q_{c_r}(k) \\ &= \sum_{n=0}^{N-1} q_{c_r}[n] e^{\frac{-j2\pi kn}{N}}, \\ &= \sum_{n=0}^{N-1} \sum_{t=0}^{T_S-1} \sum_{\omega=0}^{\Omega_1-1} \sum_{c=1}^{C_1} h_{SC_{r,t,\omega}} \alpha_{2c_1-1}^{t} b_t[n-\omega] |b_t[n-\omega]|^{2(c-1)} \\ &\quad \times e^{\frac{-j2\pi kn}{N}} + v_{c_r}(k) + w_{c_r}(k). \end{aligned} \tag{32}$$

Using circular shift property of DFT,

$$\begin{aligned} q_{c_r}(k) &= \sum_{t=0}^{T_S-1} \sum_{\omega=0}^{\Omega_1-1} h_{SC_{r,t,\omega}} \sum_{n=0}^{N-1} \sum_{c=1}^{C_1} \alpha_{2c-1}^{t} b_t[n] |b_t[n]|^{2(c-1)} \\ &\quad \times e^{\frac{-2\pi k(n+\omega)}{N}} + v_{c_r}(k) + w_{c_r}(k), \qquad (33) \\ &= \sum_{t=0}^{T_S-1} \hat{h}_{SC_{r,t,k}} \zeta_{SC}(k) + v_{c_r}(k) + w_{c_r}(k). \qquad (34) \end{aligned}$$

where,

$$\hat{h}_{SC_{r,t,k}} = \sum_{\omega=0}^{\Omega_1-1} h_{SC_{r,t,\omega}} e^{\frac{-2\pi k\omega}{N}}. \tag{35}$$

$\zeta_{SC}(k)$ is the effective nonlinear complex data symbol and is given by,

$$\zeta_{SC(k)} = \sum_{n=0}^{N-1} \alpha_{2c_1-1}^{t} \bar{\mathbf{b}}[\mathbf{n}] |\bar{\mathbf{b}}[\mathbf{n}]|^{2(c_1-1)} e^{\frac{-j2\pi kn}{N}}, \tag{36}$$

which can also be written as,

$$\zeta_{SC_t}(k) = \mu_{SC_t} a_t(k) + \gamma_{SC_t}, \tag{37}$$

where, μ_{SC_t} is the multiplicative factor due to the gain provided by the HPA at DT, and γ_{SC_t} is the additive residual noise due to the non-linearity of HPA at DT. Considering μ_{SC_t} as an unknown parameter, we express it as:

$$\mathrm{E}[\zeta_{SC_t}(k) a_t{}^*(k)] = \mu_{SC_t} P_s \tag{38}$$

Substituting ζ_{SC_t} from (36), we get:

$$\begin{aligned} \mathrm{E}[\zeta_{SC_t}(k) a_t{}^*(k)] = \mathrm{E}\Bigg[& \sum_{n=0}^{N-1} \alpha_{2c_1-1}^{t} \bar{b}_t[n] |\bar{b}_t[n]|^{2c_1-1} \\ & \times e^{\frac{-j2\pi kn}{N}} a_t{}^*(k) \Bigg]. \end{aligned} \tag{39}$$

Substituting $\bar{b}_t[n] e^{\frac{-j2\pi kn}{N}}$ from (1), we get:

$$\begin{aligned} & \mathrm{E}[\zeta_{SC_t}(k) a_t{}^*(k)] \\ &= \mathrm{E}\left[\frac{1}{N} \sum_{n=0}^{N-1} \alpha_{2c_1-1}^{t} |\bar{b}_t[n]|^{2c_1-1} a_t(k) \times a_t{}^*(k) \right] \sqrt{P_s} \\ &= \frac{(P_s)^{\frac{3}{2}}}{N} \mathrm{E}\left[\frac{1}{N} \sum_{n=0}^{N-1} \alpha_{2c_1-1}^{t} |\bar{b}_t[n]|^{2c_1-1} \right]. \end{aligned} \tag{40}$$

From (38) and (40), we get μ_{SC_t} as:

$$\mu_{SC_t} = \frac{\sqrt{P_s}}{N} \mathrm{E}\left[\frac{1}{N} \sum_{n=0}^{N-1} \alpha_{2c_1-1}^{t} |\bar{b}_t[n]|^{2c_1-1} \right]. \tag{41}$$

From (37) and (41), we obtain the expression of γ_{SC_t} as:

$$\begin{aligned} \gamma_{SC_t} = & \left(\sum_{n=0}^{N-1} \alpha_{2c_1-1}^{t} |\bar{b}_t[n]|^{2c_1-1} \right. \\ & \left. - \mathrm{E}\left[\sum_{n=0}^{N-1} \alpha_{2c_1-1}^{t} |\bar{b}_t[n]|^{2c_1-1} \right] \right) \times \bar{b}_t[n] e^{\frac{-j2\pi kn}{N}}. \end{aligned} \tag{42}$$

Thus,

$$q_{c_r}(k) = \sum_{t=0}^{T_S-1} \hat{h}_{SC_{r,t,k}} (\mu_{SC_t} a_t(k) + \gamma_t) + v_{c_r}(k) + w_{c_r}(k). \tag{43}$$

Using zero forcing equalization, the t^{th} complex data symbol at k^{th} subcarrier can be estimated as:

$$\hat{a}_t(k) = \mu_{SC_t} a_t(k) + \gamma_t + [(\hat{\mathbf{H}}_{\mathbf{SC}}(\mathbf{k}))^{+} (v_c(k) + w_c(k))]^t. \tag{44}$$

SDNR for k^{th} subcarrier at CU is given by,

$$\begin{aligned} \rho_{t_{SC}}(k) &= \frac{P_s |\mu_{SC_t}|^2}{\sigma_{\gamma_t}^2 + [((\mathbf{H}_{\mathbf{SC}})^H \mathbf{H}_{\mathbf{SC}})^{-1}]^t (N_o + \beta P_c^{\lambda})}, \\ &= \frac{\frac{P_s}{N_o + \beta P_c^{\lambda}}}{\frac{\sigma_{\gamma_t}^2}{N_o + \beta P_c^{\lambda}} + \frac{1}{\psi_{SC}}} |\mu_t|^2. \end{aligned} \tag{45}$$

B. BETWEEN CU AND DR

1) TRANSMIT SIGNAL AT CU

After decoding $\hat{a}(k)$, CU forms a broadcasting signal with power $P_c = 0.8 P_s$ as

$$\bar{\mathbf{x}}_{\mathbf{c}}[\mathbf{n}] = \hat{\mathbf{a}}[\mathbf{n} - \mathbf{n_0}], \tag{46}$$

where, n_o is the processing delay and $\hat{\mathbf{a}}[\mathbf{n}]$ is the decoded message vector received from DT.

2) NON-LINEAR HPA

$\bar{\mathbf{y}}_{\mathbf{c}}[\mathbf{n}]$ is the non-linear polynomial representing the non-linearity introduced into the OFDM modulated signal, $\bar{\mathbf{x}}_{\mathbf{c}}[\mathbf{n}]$ and is given as:

$$\bar{\mathbf{y}}_{\mathbf{c}}[\mathbf{n}] = \sum_{c_2=1}^{C_2} \alpha_{2c_2-1}^{t} \bar{\mathbf{x}}_{\mathbf{c}}[\mathbf{n}] |\bar{\mathbf{x}}_{\mathbf{c}}[\mathbf{n}]|^{2(c_2-1)} \quad 1 \le t \le T_2, \tag{47}$$

where, $\bar{\mathbf{y}}_{\mathbf{c}}[\mathbf{n}]$ is a $T_R \times 1$ vector of transmit signals at CU.

The received signal vector $\bar{\mathbf{q}}_{\mathbf{D}}[\mathbf{n}]$ at DR, can be written as,

$$\bar{\mathbf{q}}_{\mathbf{D}}[\mathbf{n}] = \mathbf{H}_{\mathbf{2}_{\omega}} \bar{\mathbf{y}}_{\mathbf{c}}[\mathbf{n}] + \bar{\mathbf{w}}_{\mathbf{D}}[\mathbf{n}]. \tag{48}$$

The complex data symbol at the r^{th} receive antenna at DR can be written as:

$$q_{D_r}[n] = \sum_{t=0}^{T_R-1}\sum_{\omega=0}^{\Omega_2-1}\sum_{c_2=1}^{C_2} h_{CD_{r,t,\omega}}\alpha^t_{2c_2-1}\overline{x}_c[n-\omega]| \times \overline{x}_c[n-\omega]|^{2(c-1)} + w_{D_r}[n]. \quad (49)$$

After the removal of the CP and applying DFT,

$$\begin{aligned} &q_{D_r}(k) \\ &= \sum_{n=0}^{N-1} q_{D_r}[n]e^{\frac{-j2\pi kn}{N}}, \\ &= \sum_{n=0}^{N-1}\sum_{t=0}^{T_R-1}\sum_{\omega=0}^{\Omega_2-1} h_{CD_{r,t,\omega}}\alpha^t_{2c_2-1}\overline{x}_c[n-\omega]|\overline{x}_c[n-\omega]|^{2(c_2-1)} \\ &\quad \times e^{\frac{-j2\pi kn}{N}} + w^r_D(k). \end{aligned} \quad (50)$$

Using circular shift property of DFT,

$$\begin{aligned} q_{D_r}(k) &= \sum_{t=0}^{T_R-1}\sum_{\omega=0}^{\Omega_2-1} h_{CD_{r,t,\omega}}\sum_{n=0}^{N-1}\alpha^t_{2c-1}\overline{x}_c[n]|\overline{x}_c[n]|^{2(c-1)} \\ &\quad \times e^{\frac{-2\pi k(n+\omega)}{N}} + w^r_D(k), \\ &= \sum_{t=0}^{T_R-1}\hat{h}_{CD_{r,t,k}}\zeta_{CD}(k) + w_{D_r}(k), \end{aligned} \quad (51)$$

$\zeta_{CD}(k)$ is the effective nonlinear complex data symbol and is given by,

$$\zeta_{CD}(k) = \sum_{n=0}^{N-1}\alpha^t_{2c_2-1}\overline{x}_c[n]|\overline{x}_c[n]|^{2(c_2-1)}e^{\frac{-j2\pi kn}{N}}, \quad (52)$$

which can also be written as,

$$\zeta_{CD}(k) = \mu_{CD_t}\hat{a}(k) + \gamma_{CD_t}, \quad (53)$$

where, μ_{CD_t} and γ_{CD_t} are the multiplicative factor due to the gain provided by the HPA at CU and the additive residual noise due to the non-linearity of HPA at CU respectively, and are given as:

$$\mu_{CD_t} = \frac{\sqrt{P_c}}{N}\mathrm{E}\left[\frac{1}{N}\sum_{n=0}^{N-1}\alpha^t_{2c_2-1}|\overline{b_t}[n]|^{2c_2-1}\right]. \quad (54)$$

$$\begin{aligned} \gamma_{CD_t} &= \left(\sum_{n=0}^{N-1}\alpha^t_{2c_2-1}|\overline{b}_t[n]|^{2c_2-1}\right. \\ &\quad \left. - \mathrm{E}\left[\sum_{n=0}^{N-1}\alpha^t_{2c_2-1}|\overline{b}_t[n]|^{2c_2-1}\right]\right) \times \overline{b}_t[n]e^{\frac{-j2\pi kn}{N}}. \end{aligned} \quad (55)$$

Thus,

$$q_{D_r}(k) = \sum_{t=0}^{T_R-1}\hat{h}_{CD_{r,t,k}}(\mu_t\hat{a}(k) + \gamma(t)) + w_{D_r}(k). \quad (56)$$

TABLE 2. Non-linear coefficients used in simulation.

Coefficient	Value
α_1 between DT and CU	$0.9955 + 0.0120i$
α_3 between DT and CU	$-0.2208 + 0.1717i$
α_1 between CU and DR	$0.9559 + 0.0210i$
α_3 between CU and DR	$-0.2802 + 0.1771i$

Using zero forcing equalization, the t^{th} complex data symbol at k^{th} subcarrier can be estimated as:

$$\tilde{a}(k) = \mu_{CD_t}\hat{a}(k) + \gamma_t + [(\hat{\mathbf{H}}_{\mathbf{CD}}(\mathbf{k}))^{\dagger}w_D(k)]^t. \quad (57)$$

SDNR between CU and DR is:

$$\begin{aligned} \rho_{t_{CD}}(k) &= \frac{P_c|\mu_t|^2}{\sigma^2_{\gamma CD_t} + [((\mathbf{H_{CD}})^H\mathbf{H_{CD}})^{-1}]^tN_o}, \\ &= \frac{\frac{P_c}{N_o}}{\frac{\sigma^2_{\gamma_t}}{N_o} + \frac{1}{\psi_{CD}}}|\mu_{CD_t}|^2. \end{aligned} \quad (58)$$

The SER can be calculated using the expression given in (28) and (58).

V. SIMULATION RESULTS

In this section, the SER performance of the MIMO-OFDM based FD C-D2D system with $N = 2048$ subcarriers and $N_{CP} = 512$ is evaluated for the transmission between DT-CU and CU-DR. Each MIMO-OFDM subcarrier contains complex data symbols from M-QAM constellation, where $M = 16$. The Rayleigh fading channels have been represented by the six delay taps each, i.e, $\Omega_1 = 6$ and $\Omega_2 = 6$ with uniform power delay profile [22]. $\beta = 1.5$ and $\lambda = 0.5$ have been considered as the parameters for determining the performance of SIC in Fig. 4 and Fig. 5. The values of the complex non-linearity coefficients, α_1 and α_3, used to model the non-linear HPA for transmission between DT and CU and between CU and DR, are given in Table 2. For linear HPA, $\alpha_1 = 1$ and $\alpha_3 = 0$. We have considered $P_c = 0.8P_s$ for our simulation purpose. For the SER analysis of Fig. 4 to Fig. 7, we have considered $d_{SC} = 100$m and $d_{CU} = 100$m as the distance between DT and CU, and the distance between CU and DR, respectively.

The performance comparison in terms of SER for linear and non-linear HPA with different IBOs has been shown in Fig. 4 and Fig. 5. Specifically, Fig. 4 shows the SER comparison for transmission between DT and CU. In contrast, Fig. 5 shows the SER comparison for transmission between CU and DR. Here, IBO is defined as the ratio of OFDM average power (P_{sat}) to the input voltage (P_{inp}) applied to HPA [22].

From Fig. 4, we observe that an ideal MIMO-OFDM FD C-D2D system with linear HPA and zero RSI outperforms all the other scenarios. At lower SNR values, the AWGN dominates over RSI, which leads to an identical performance of the two systems, with and without RSI. As the SNR increases, the dominance of AWGN reduces,

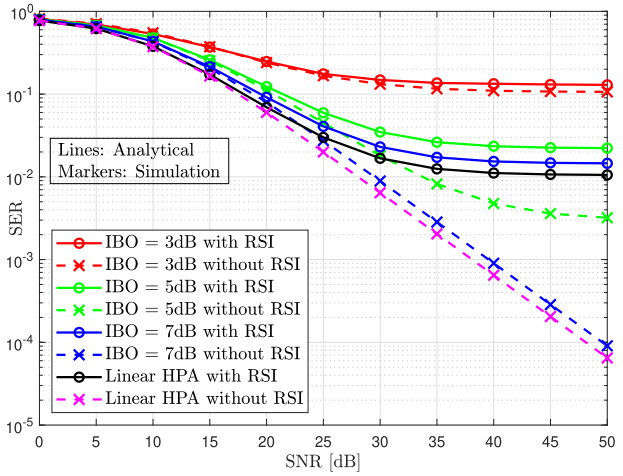

FIGURE 4. Comparison of performance for different IBO in transmission between DT and CU.

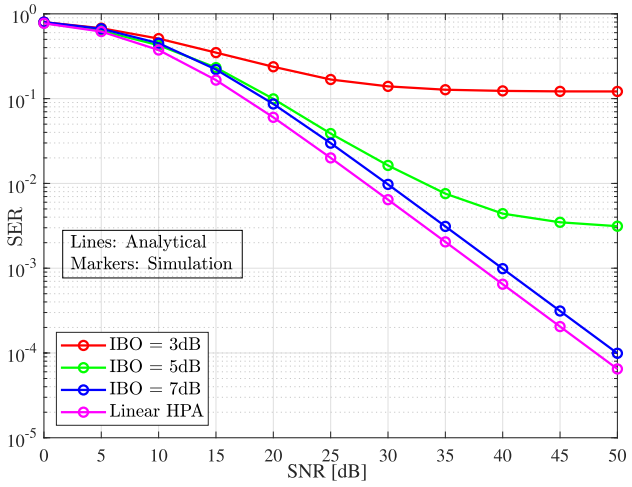

FIGURE 5. Comparison of performance for different IBO in transmission between CU and DR.

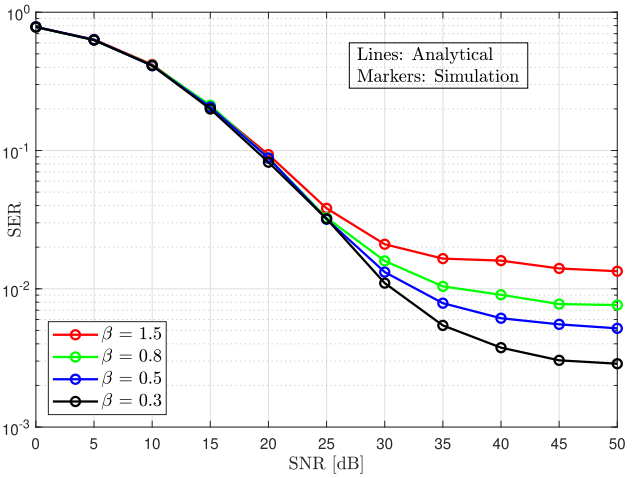

FIGURE 6. Comparison of performance with different β in transmission between DT and CU for non-linear HPA.

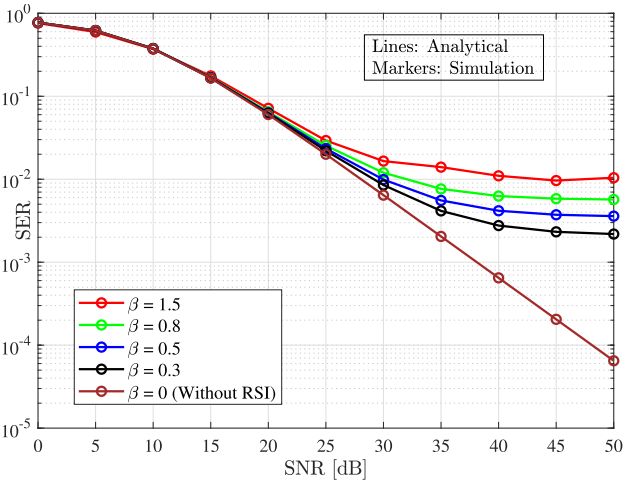

FIGURE 7. Comparison of performance with different β in transmission between DT and CU for linear HPA.

and the difference between the performances of the systems can be easily distinguished. As far as the non-linear MIMO-OFDM FD C-D2D system is concerned, it can be observed that the performance of these systems improves as the IBO increases. The increase in IBO makes the non-linear HPA behave as a linear HPA resulting in an improvement in the performance of the system. For instance, at SNR $=$ 50 dB, SER for IBO $= 3, 5, 7$ dB with RSI is 1.293×10^{-1}, 2.225×10^{-2},and 1.457×10^{-2}, respectively, whereas SER for linear HPA with RSI is 1.055×10^{-2}. Hence, we can conclude that IBO $=$ 7 dB has the closest performance to linear HPA. Further, from Fig. 4, it can be observed that as the IBO increases, the dominance of the non-linearity reduces over RSI, and the difference in the performance of the systems with and without RSI can be easily distinguished. For instance, at SNR $=$ 50 dB, SER for IBO $= 3, 5, 7$ dB without RSI is 1.065×10^{-1}, 3.201×10^{-3}, and 9.073×10^{-5}, respectively, whereas SER for linear HPA without RSI is 6.477×10^{-5}.

Fig. 5 represents the SER performance for transmission between CU and DR. Here, we can observe that increasing IBO will improve the SER for non-linear HPA.

Fig. 6 represents the SER performance with respect to SNR while varying the RSI parameter β, as 1.5, 0.8, 0.5, and 0.3 with a fixed IBO of 7 dB for non-linear HPA. It can be observed from Fig. 6 that as the value of β decreases, its impact on the SER performance reduces. This is due to the fact that with a decrement in β, RSI reduces, and it becomes less dominant compared to AWGN. For instance, $\beta = 1.5$ has a higher SER than $\beta = 0.8$ for all values of SNR from 0 dB to 50 dB. Fig. 7 shows the SER performance for FD C-D2D system with linear HPA with RSI (for the same values of β as considered in Fig. 6) and without RSI (in an ideal FD C-D2D system). It is evident from Fig. 6 and Fig. 7 that the SER performance of the FD C-D2D system with linear HPA is better than its counterpart with non-linear HPA. A comparison in the SER performance in Fig. 6 and Fig. 7 for all SNR values from 0 dB to 50 dB shows that the SER performance of the linear MIMO-OFDM FD C-D2D system

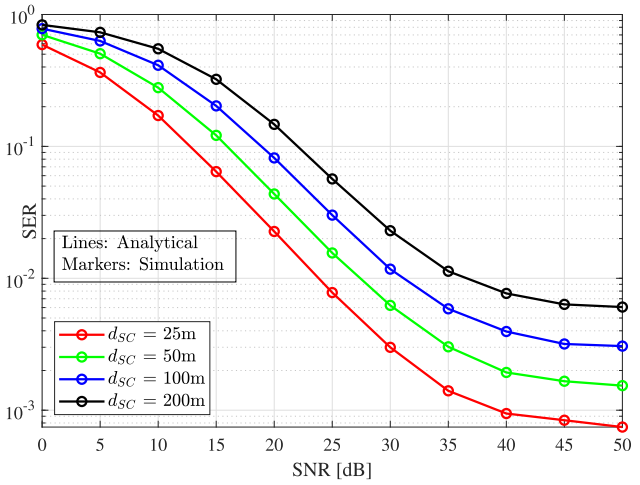

FIGURE 8. Comparison of SER performance with varying distance between DT and CU.

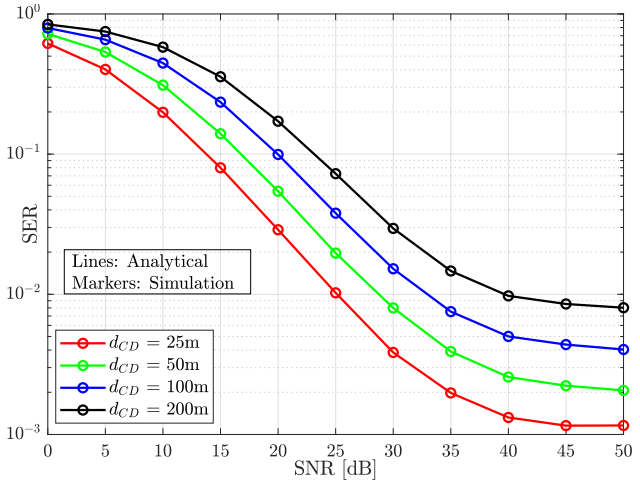

FIGURE 9. Comparison of SER performance with varying distance between CU and DR.

is better than that of the non-linear MIMO-OFDM FD C-D2D system.

Fig. 8 represents the SER performance of DT-CU link with respect to SNR for different values of the distances between DT and CU (d_{SC}) using a nonlinear HPA with IBO = 7 dB and $\beta = 0.3$. From Fig. 8, we can observe that as d_{SC} increases, the SER decreases. For instance, when SNR = 35 dB, SER for $d_{SC} = \{25, 50, 100, 200\}$ m is 1.4028×10^{-3}, 3.0244×10^{-3}, 5.8705×10^{-3}, and 1.1307×10^{-2}, respectively. Similarly, Fig. 9 represents the SER performance of CU-DR link for different values of distances between CU and DR (d_{CD}) using a nonlinear HPA with IBO = 7 dB and $\beta = 0.3$. A similar trend can be observed from Fig. 9, where the SER performance degrades as d_{CD} increases. For instance, when SNR = 35 dB, SER for $d_{CD} = \{25, 50, 100, 200\}$ m is 1.9792×10^{-3}, 3.9073×10^{-3}, 7.5238×10^{-3}, and 1.4676×10^{-2}, respectively. This shows that as the distance between the devices, i.e., d_{SC} or d_{CD} increases, the SER also increases. Hence, it can be concluded that C-D2D is more effective when the distances between the devices (DT-CU or CU-DR) are less.

VI. CONCLUSION

This paper proposed a MIMO-OFDM based FD C-D2D system, where a CU acts as an FDR for D2D transmission. Closed-form expressions of SER for DT-CU and CU-DR transmissions have been derived in the form of a joint polynomial model for the non-linear MIMO-OFDM system. Further, the obtained results are compared with a linear MIMO-OFDM system. Moreover, we have shown that the proposed framework works similarly to a linear MIMO-OFDM based FD C-D2D system by using IBO. We have also shown that if RSI gets reduced, then its adverse effects on the performance of the system also get reduced. As the FD D2D system helps in improving spectral efficiency, the proposed framework will be helpful in achieving higher spectral efficiency with good reliability of transmission. As a future direction, the proposed analysis can be further extended to non-linear MU-MIMO OFDM-based FD systems and CA long-term evolution advanced (LTE-A) based FD systems.

REFERENCES

[1] J. Fiaidhi and S. Mohammed, "Internet of everything as a platform for extreme automation," *IT Prof.*, vol. 21, no. 1, pp. 21–25, Jan. 2019.
[2] Z. Nezami and K. Zamanifar, "Internet of Things/Internet of Everything: Structure and ingredients," *IEEE Potentials*, vol. 38, no. 2, pp. 12–17, Mar. 2019.
[3] L. Chettri and R. Bera, "A comprehensive survey on Internet of Things (IoT) toward 5G wireless systems," *IEEE Internet Things J.*, vol. 7, no. 1, pp. 16–32, Jan. 2020.
[4] H. Song, Q. Cui, Y. Gu, G. L. Stüber, Y. Li, Z. Fei, and C. Guo, "Cooperative LBT design and effective capacity analysis for 5G NR ultra dense networks in unlicensed spectrum," *IEEE Access*, vol. 7, pp. 50265–50279, 2019.
[5] S. Kumar, A. S. Dixit, R. R. Malekar, H. D. Raut, and L. K. Shevada, "Fifth generation antennas: A comprehensive review of design and performance enhancement techniques," *IEEE Access*, vol. 8, pp. 163568–163593, 2020.
[6] S. Sharma, N. Gupta, and V. A. Bohara, "OFDMA-based device-to-device communication frameworks: Testbed deployment and measurement results," *IEEE Access*, vol. 6, pp. 12019–12030, 2018.
[7] W.-K. Lai, Y.-C. Wang, H.-C. Lin, and J.-W. Li, "Efficient resource allocation and power control for LTE-A D2D communication with pure D2D model," *IEEE Trans. Veh. Technol.*, vol. 69, no. 3, pp. 3202–3216, Mar. 2020.
[8] R. I. Ansari, C. Chrysostomou, S. A. Hassan, M. Guizani, S. Mumtaz, J. Rodriguez, and J. J. P. C. Rodrigues, "5G D2D networks: Techniques, challenges, and future prospects," *IEEE Syst. J.*, vol. 12, no. 4, pp. 3970–3984, Dec. 2018.
[9] N. Gupta and V. A. Bohara, "Rate and outage trade-offs for OFDMA based device to device communication frameworks," *IEEE Access*, vol. 5, pp. 14095–14106, 2017.
[10] P. Khuntia, R. Hazra, and P. Goswami, "A bidirectional relay-assisted underlay device-to-device communication in cellular networks: An IoT application for FinTech," *IEEE Internet Things J.*, early access, Jun. 11, 2021, doi: 10.1109/JIOT.2021.3088539.
[11] H. Nourizadeh, S. Nourizadeh, and R. Tafazolli, "Performance evaluation of cellular networks with mobile and fixed relay station," in *Proc. IEEE Veh. Technol. Conf.*, Sep. 2006, pp. 1–5.
[12] Y. Chen, B. Ai, Y. Niu, Z. Han, R. He, Z. Zhong, and G. Shi, "Sub-channel allocation for full-duplex access and device-to-device links underlaying heterogeneous cellular networks using coalition formation games," *IEEE Trans. Veh. Technol.*, vol. 69, no. 9, pp. 9736–9749, Sep. 2020.
[13] C. D. Nwankwo, L. Zhang, A. Quddus, M. A. Imran, and R. Tafazolli, "A survey of self-interference management techniques for single frequency full duplex systems," *IEEE Access*, vol. 6, pp. 30242–30268, 2018.
[14] F. J. Soriano-Irigaray, J. S. Fernandez-Prat, F. J. Lopez-Martinez, E. Martos-Naya, O. Cobos-Morales, and J. T. Entrambasaguas, "Adaptive self-interference cancellation for full duplex radio: Analytical model and experimental validation," *IEEE Access*, vol. 6, pp. 65018–65026, 2018.

[15] S. B. Venkatakrishnan, E. A. Alwan, and J. L. Volakis, "Wideband RF self-interference cancellation circuit for phased array simultaneous transmit and receive systems," *IEEE Access*, vol. 6, pp. 3425–3432, 2018.

[16] M. S. Sim, K. S. Kim, and C.-B. Chae, "Self-interference cancellation for LTE-compatible full-duplex systems," in *Proc. IEEE Int. Conf. Commun. Workshops (ICC Workshops)*, May 2018, pp. 1–6.

[17] A. Masmoudi and T. Le-Ngoc, "Residual self-interference after cancellation in full-duplex systems," in *Proc. IEEE Int. Conf. Commun. (ICC)*, Jun. 2014, pp. 4680–4685.

[18] I. Budhiraja, N. Kumar, S. Tyagi, S. Tanwar, and M. Guizani, "SWIPT-enabled D2D communication underlaying NOMA-based cellular networks in imperfect CSI," *IEEE Trans. Veh. Technol.*, vol. 70, no. 1, pp. 692–699, Jan. 2021.

[19] R. Bajpai, N. Gupta, and V. A. Bohara, "An adaptive full-duplex/half-duplex multiuser cooperative D2D communications system with best user selection," *IEEE Open J. Commun. Soc.*, vol. 2, pp. 1445–1457, 2021.

[20] Y. Du, J. Liu, and Y. Chen, "Performance analysis of nonlinear SFBC OFDM systems over TWDP fading channel," *IEEE Access*, vol. 7, pp. 101981–101991, 2019.

[21] P. Aggarwal, A. Pradhan, and V. A. Bohara, "A downlink multiuser MIMO–OFDM system with nonideal oscillators and amplifiers: Characterization and performance analysis," *IEEE Syst. J.*, vol. 15, no. 1, pp. 715–726, Mar. 2021.

[22] P. Aggarwal and V. A. Bohara, "End-to-end theoretical evaluation of a nonlinear MIMO-OFDM system in the presence of digital predistorter," *IEEE Syst. J.*, vol. 13, no. 3, pp. 2309–2319, Sep. 2019.

[23] G. Liu, W. Feng, Z. Han, and W. Jiang, "Performance analysis and optimization of cooperative full-duplex D2D communication underlaying cellular networks," *IEEE Trans. Wireless Commun.*, vol. 18, no. 11, pp. 5113–5127, Nov. 2019.

[24] S. Dang, G. Chen, and J. P. Coon, "Multicarrier relay selection for full-duplex relay-assisted OFDM D2D systems," *IEEE Trans. Veh. Technol.*, vol. 67, no. 8, pp. 7204–7218, Aug. 2018.

[25] N. Gupta, D. Kumar, and V. A. Bohara, "A novel user selection and resource allocation framework for cooperative D2D communication," in *Proc. IEEE Global Commun. Conf. (GLOBECOM)*, Dec. 2018, pp. 1–7.

[26] R. Bajpai, A. Kulkarni, G. Malhotra, and N. Gupta, "Outage analysis of OFDMA based NOMA aided full-duplex cooperative D2D system," in *Proc. 27th Int. Conf. Telecommun. (ICT)*, Oct. 2020, pp. 1–5.

[27] J. Lee and J. H. Lee, "Performance analysis and resource allocation for cooperative D2D communication in cellular networks with multiple D2D pairs," *IEEE Commun. Lett.*, vol. 23, no. 5, pp. 909–912, May 2019.

[28] S. Parvez, P. K. Singya, and V. Bhatia, "On ASER analysis of energy efficient modulation schemes for a device-to-device MIMO relay network," *IEEE Access*, vol. 8, pp. 2499–2512, 2020.

[29] Y. Liu, C. Pan, L. You, and W. Han, "D2D-enabled user cooperation in massive MIMO," *IEEE Syst. J.*, vol. 14, no. 3, pp. 4406–4417, Sep. 2020.

[30] P. Aggarwal and V. A. Bohara, "A nonlinear downlink multiuser MIMO-OFDM systems," *IEEE Wireless Commun. Lett.*, vol. 6, no. 3, pp. 414–417, Jun. 2017.

[31] H. Moazzen, A. Mohammadi, and M. Majidi, "Performance analysis of linear precoded MU-MIMO-OFDM systems with nonlinear power amplifiers and correlated channel," *IEEE Trans. Commun.*, vol. 67, no. 10, pp. 6753–6765, Oct. 2019.

[32] P. Aggarwal and V. A. Bohara, "Analytical characterization of dual-band multi-user MIMO-OFDM system with nonlinear transmitter constraints," *IEEE Trans. Commun.*, vol. 66, no. 10, pp. 4536–4549, Oct. 2018.

[33] B. C. Nguyen, P. V. Tri, X. N. Tran, and L. T. Dung, "SER performance of MIMO full-duplex relay system with channel estimation errors and transceivers hardware impairments," *Int. J. Electron. Commun.*, vol. 136, Jul. 2021, Art. no. 153751.

[34] T. Araujo and R. Dinis, "Analytical evaluation of nonlinear effects on OFDMA signals," *IEEE Trans. Wireless Commun.*, vol. 9, no. 11, pp. 3472–3479, Nov. 2010.

[35] T. Araujo and R. Dinis, "On the accuracy of the Gaussian approximation for the evaluation of nonlinear effects in OFDM signals," *IEEE Trans. Commun.*, vol. 60, no. 2, pp. 346–351, Feb. 2012.

[36] J. Guerreiro, R. Dinis, and P. Montezuma, "Analytical performance evaluation of precoding techniques for nonlinear massive MIMO systems with channel estimation errors," *IEEE Trans. Commun.*, vol. 66, no. 4, pp. 1440–1451, Apr. 2018.

[37] J. Guerreiro, R. Dinis, and P. Montezuma, "Equivalent nonlinearities for studying nonlinear effects on sampled OFDM signals," *IEEE Commun. Lett.*, vol. 19, no. 4, pp. 529–532, Apr. 2015.

[38] A. Papoulis, *Probability, Random Variables Stochastic Processes*. New York, NY, USA: McGraw-Hill, 1965.

[39] M. H. N. Shaikh, V. A. Bohara, P. Aggarwal, and A. Srivastava, "Energy efficiency evaluation for downlink full-duplex nonlinear MU-MIMO-OFDM system with self-energy recycling," *IEEE Syst. J.*, vol. 14, no. 3, pp. 3313–3324, Sep. 2020.

[40] P. Aggarwal and V. A. Bohara, "On the multiband carrier aggregated nonlinear LTE-A system," *IEEE Access*, vol. 5, pp. 16930–16943, 2017.

[41] H. Chour, E. A. Jorswieck, F. Bader, Y. Nasser, and O. Bazzi, "Global optimal resource allocation for efficient FD-D2D enabled cellular network," *IEEE Access*, vol. 7, pp. 59690–59707, 2019.

[42] L. Han, Y. Zhang, Y. Li, and X. Zhang, "Spectrum-efficient transmission mode selection for full-duplex-enabled two-way D2D communications," *IEEE Access*, vol. 8, pp. 115982–115991, 2020.

[43] R. Bajpai and N. Gupta, "Outage trade-offs between full/half-duplex relaying for NOMA aided multicarrier cooperative D2D communications system," *IETE Tech. Rev.*, vol. 38, pp. 1–13, Sep. 2021.

MANISH DASH received the B.E. degree in electronics and communication engineering from BITS Pilani, K. K. Birla Goa Campus, Goa, India, in 2021. Currently, he is working with the HDD Research and Development Department, Western Digital. His research interests include device-to-device communications, full duplex communications, massive MIMO, filter design, and signal processing.

RAHUL BAJPAI received the M.Tech. degree in digital communication from ABV-IIITM, Gwalior, India, in 2014. He is currently pursuing the Ph.D. degree with the Department of Electrical and Electronics Engineering, BITS Pilani, K. K. Birla Goa Campus, India. His research interests include 6G technologies, non-orthogonal multiple access, full-duplex radio, millimeter-wave, device-to-device communication, and machine learning for wireless communications. He has served as a Reviewer for the *Wireless Networks* (Springer) and *Wireless Personal Communications* (Springer).

NAVEEN GUPTA received the M.Tech. degree in advanced communication systems from NIT-Warangal, in 2011, and the Ph.D. degree in wireless communications from IIIT-Delhi, India, in 2017. He is currently working as an Assistant Professor with the Department of EEE, BITS Pilani, K. K. Birla Goa Campus, India. His research interests include resource allocations for next generation wireless communication techniques, non-orthogonal multiple access, full-duplex, millimeter-wave, and device-to-device communication. He has served as a Reviewer for the IEEE Transactions on Cognitive Communications and Networking, IEEE Transactions on Communications, IEEE Access, and the IEEE Transactions on Wireless Communications.

PARAG AGGARWAL (Member, IEEE) received the Ph.D. degree from IIIT-Delhi, India, in 2019. He joined Wipro Ltd., in 2019, as a 5G Architect. Currently, he is working with the 5G Research and Development Laboratory, HFCL Ltd. His research interests include O-RAN, waveform designing, massive MIMO, carrier/spectrum aggregation, nonlinear modeling, digital predistortion techniques, and RF power amplifiers.